

Correlating Nanostructures with Function: Structural Colors on the Wings of a Malaysian Bee

Matin T.R.¹, Leong M.K.², Majlis B.Y.¹ and Gebeshuber I.C.^{1,3*}

¹ *Institute of Microengineering and Nanoelectronics, Universiti Kebangsaan Malaysia,
43600 UKM, Bangi, Selangor, Malaysia*

² *Crest Nano Solution (M) Sdn. Bhd., Jalan Puchong, 47100 Puchong, Malaysia*

³ *Institute of Applied Physics, Vienna University of Technology,
Wiedner Hauptstrasse 8-10/134, 1040 Wien, Austria*

Abstract. Structural colours refer to colours generated by nanostructures, with the characteristic dimension of the structures on the wavelength of the visible light (i.e., some hundreds of nanometers). Examples for structural colours are the colours of CDs and DVDs, the colours of soap bubbles or oil films on water (thin films), or the colours of certain butterfly wings (e.g., photonic crystals). Recently, we located a Malaysian bee with iridescent structural coloration on its wings. The generation of the colouration is still unknown, and there is no respective scientific literature available. This study presents the first AFM experiments related to the structural coloration of the carpenter bee wing. First attempts to investigate the nanostructures of the wing were performed with non-contact atomic force microscopy (AFM, Park Systems XE-100), using a Silicon nitride cantilever with a spring constant of 40 N/m and a resonance frequency of 300.000 kHz. The AFM scans reveal three layers with structures with a diameter of several hundreds of nanometres. This, rules out thin films as the structures yielding the coloration. Future research and correlation of various structures with function in this bee wings will shed light on the contribution of these structures visible in the first AFM scans to the colouration. Structural colours produced by nature inspire novel approaches in man-made colours, via biomimetics (i.e., knowledge transfer from biology to technology).

Keywords: atomic force microscopy, biomimetics, natural nanostructures, structural colours.

PACS: 61.46.-w, 78.20.-e, 78.67.-n, 81.07.-b, 87.64.Dz, 87.85.jc

INTRODUCTION

Iridescent and metallic coloration in flora and fauna is not caused by pigments, but rather by physical structures with characteristic sizes on the order of several hundreds of nanometres [1-6].

According to previous studies about various kinds of colours and their origin, colours are divided to two different categories: chemical colours and structural colours. Chemical colours are caused by pigments, whereas structural colours are caused by structures with a size of the wavelength of the visible light (i.e., some hundreds of nanometres). The interaction of visible light with structures cause shiny, bright colours that might also show iridescence (i.e., change of coloration with the viewing angle) [1-6].

In chemical colours, the light excites electrons of the pigments to higher excited states by energy consumption of light. The colour is then caused by the exchange of energy between light and electron.

In structural colours, on the other hand, incident light is reflected, scattered, and deflected on structures, with negligible energy exchange between the material and the light, resulting in strong, shiny coloration.

The objective of this paper is to discuss colour generation in structural colours, describe their physical basics, give some examples for structural colours from nature and technology and report the first research results of investigations of the colourful wing of the Malaysian carpenter bee, performed with Atomic Force Microscopy (AFM).

THE PHYSICS OF COLORS

Five physical phenomena lead to structural coloration [1]:

- thin films interference,
- multilayer interference,
- scattering,
- diffraction and photonic crystals.

1. Thin Film Interference

Thin film interference occurs when an incident light wave is partly reflected by the upper and lower boundaries of a thin film (Fig. 1). It is one of the simplest phenomena in structural coloration and can be found in various instances in nature, for example in the wings of houseflies, in oil films on water or in soap bubbles.

Light that strikes a thin film surface can be either transmitted or reflected from upper or lower boundary, respectively. This can be described by the Fresnel equation. Interference between two reflected light waves can be constructive or destructive, depending on their phase difference. Of relevance are the thickness of the film layer (d), the refractive index of the film (n) and the angle of incidence of the original wave on the film (θ_1). In addition, if the refractive index n_2 of the thin film is larger than the refractive index of the outside medium n_1 , there is a 180 degree phase shift in the reflected wave. This is for example the case in a soap bubble, with $n_1=n_{\text{air}}=1$ and $n_2=n_{\text{film}}$, with $n_{\text{air}}<n_{\text{film}}$.

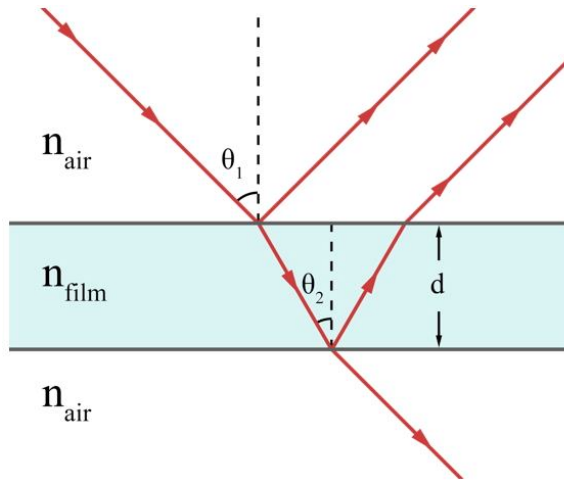


FIGURE 1. Thin film interference in the case of e.g., soap bubbles.

The reflection on the upper boundary of the film (the air-film boundary) causes a 180° phase shift in the reflected wave (since $n_{\text{air}}<n_{\text{film}}$). Light that is transmitted at this first boundary continues to the lower film-air interface, where it is either reflected or transmitted. The reflection at this boundary has no phase change because $n_{\text{film}}>n_{\text{air}}$.

The condition for constructive interference for a soap bubble is given in equation (1), the condition for destructive interference is given in equation (2):

$$2n_{\text{film}}d\cos(\theta_2) = (m - 1/2)\lambda \quad (1)$$

$$2n_{\text{film}}d\cos(\theta_2) = m\lambda \quad (2)$$

Where d equals the film thickness, n_{film} equals the refractive index of the film, θ_2 equals the angle of incidence of the wave on the lower film-air boundary, m is an integer, and λ is the wavelength of light.

Summing up, there are two conditions that should be satisfied for constructive interference: firstly, the thin film should be thin enough to crest the reflected waves and secondly, the two reflected waves should be in one phase [7].

2. Multi Layer Interference

As described above a light wave can be reflected from both boundaries of a thin film layer and dependent on the phase of two reflected light waves either destructive or constructive interference occur. The same phenomenon occurs in a series of thin films, a multilayer. A schematic of a multilayer is given in Fig. 2. With $n_B>n_A$, between each A-B interface a 180 change in phase takes place, while at the B-A interface there would be no phase change. Reflection or refraction at the surface of a medium with a lower refractive index causes no phase shift. Reflection at the surface of a medium with a higher refractive index causes a phase shift of half of a wavelength.

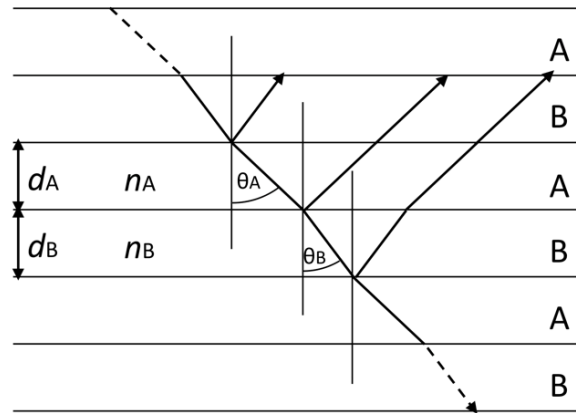


FIGURE 2. Multilayer interference. $n_B>n_A$. A change in viewing angle corresponds to a change in the perceived colour, due to changes in the phases of the interfering waves.

Constructive interference:

$$2(n_A d_A \cos \theta_A + n_B d_B \cos \theta_B) = m\lambda \quad (3)$$

Maximum reflection:

$$2n_A d_A \cos \theta_A = (m' - 1/2)\lambda \quad (4)$$

In ideal multilayers all waves interfere constructively, resulting in colourful reflections, whereas in non-ideal multilayers the waves interfere destructively and the reflection is less colourful [3, 8-10].

3. Diffraction Gratings

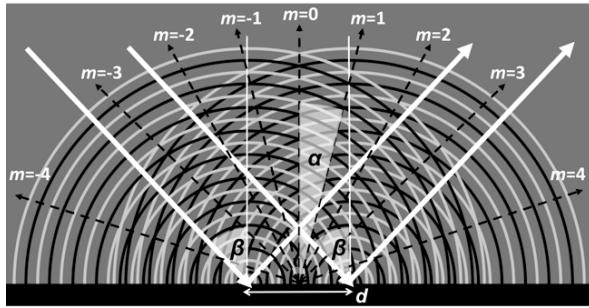


FIGURE 3. Schematic of the colour generating mechanism by the diffraction of light by a diffraction grating (black bar on bottom).

The grating equation (4) correlates the spacing of the grating (d) with the angles of the diffracted and incident beams (α , β) and the wavelengths of illuminating light (λ) (Fig. 3). The coloration in a particular direction (viewing angle) is generated by the interfering components from each slit of the grating. The diffracted light has maxima at angles where there is no phase difference between the waves. The 0th order reflection corresponds to direct transmission and is denoted $m=0$. Other maxima occur at angles with $m=\pm 1, \pm 2, \pm 3, \dots$

$$d \cdot (\sin \alpha - \sin \beta) = m \cdot \lambda \quad (1)$$

CDs and DVDs are examples for this phenomenon. It is hardly found in animated nature. The few reported examples of diffraction grating-like structures comprise hairs of crustaceans and marine worms (*Polychaeta*) [3, 8, 11].

4. Scattering

The term scattering is more general denomination for the interference of light waves with different wavelengths reflected from scattering objects either in a constructive or destructive way (Fig. 4). In terms of coloration, scattering can yield either strong or fade colours. Examples of scattering and more precisely coherent scattering are the thin film interference and the multilayer film interference described above.

In coherent scattering there is a definite phase relationship between incoming and scattered waves, whereas in incoherent scattering this is not the case.

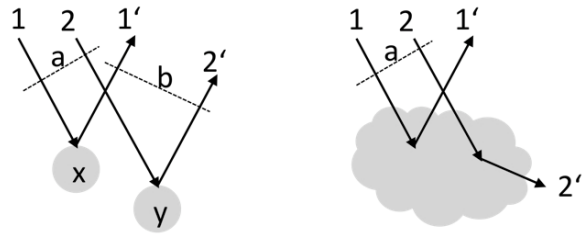


FIGURE 4. Coherent (left) and incoherent scattering (right).

The two main types of scattering are termed Rayleigh scattering and Tyndall scattering. In both types of scattering, the intensity of the scattered light depends on the fourth power of the frequency. In Rayleigh scattering, the scatter particles are much smaller than the wavelength of the incident light, whereas in Tyndall scattering, the scatter particles are macroscopic (e.g., dust particles or small fat particles in water, as in milk). Since blue light (i.e., shorter wavelengths) is scattered more than red light (i.e., long wavelengths), milk, tobacco smoke and the sky are blue or have a blue hue. In animated nature, for example the blue of some butterflies can be explained by scattering [12]. Multiple scattering within regular structures produces highly reflective bands in the reflection spectrum, and leads to the brilliant colours observed, e.g., in various butterflies [1].

5. Photonic Crystals

Photonic crystals exhibit a nanoscale periodicity a in the refractive index (Fig. 5). There are one-, two- and three-dimensional photonic crystals. Depending on their wavelength, photons either can be transmitted through the crystal or not (allowed and forbidden energy bands) [13, 14]. For effects in the visible range, the periodicity of the photonic crystal has to be of the between about 200 nm (blue) and 350 nm (red).

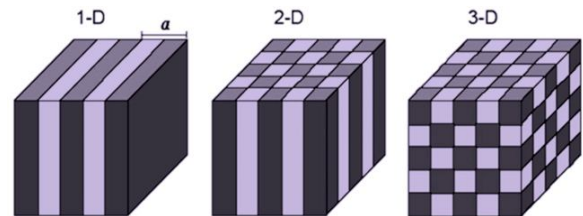


FIGURE 5. Schematics of one-, two- and three-dimensional photonic crystals (1-D, 2-D, 3-D). The colours represent materials with different refractive indices. The spatial period of the material is called the lattice constant, a .

FLORA AND FAUNA WITH STRUCTURAL COLORS

Structural colours are found in various animals, plants and microorganisms [1].

Studies of structural colours date back to 17th century when the oldest scientific description on the structural colours appeared in “Micrographia”, written by Robert Hooke in 1665 [15].

In “Opticks” [16], Sir Isaac Newton related iridescence (i.e., the change in observed color with viewing angle) to optical interference:

‘The finely colour’d feathers of some birds, and particularly those of the peacocks’ tail, do in the very same part of the feather appear of several colours in several positions of the eye, after the very same manner that thin plates were found to do.’

Since then, various organisms with structural colours, including butterflies and moths, beetles and other insects, birds and fishes have been reported. In this section, a few of them are introduced, along with a description of the physical phenomena and structures causing the coloration.

Butterflies and Moths

“Butterflies and moths are probably the most conspicuous and attractive group in insects and it has been source of people’s inspiration in artistic and scientific activities since beginning of civilization.” [1]

Different types of physical mechanisms, including multilayer interference, diffraction, Bragg scattering, Tyndall scattering and Rayleigh scattering can be found in structural colour mechanism of butterflies and moths [17].

Morpho butterflies (Fig. 6 and 7) are one of the most familiar iridescent creatures have been extensively studied for over a century. The colours are generated by Christmas tree-like structures, whose characteristic dimensions are a couple of hundreds of nanometres (Fig. 7).

Transmission electron microscopy of wing-scale cross-sections of *M. rhetenor* (Fig. 7b) and *M. didius* (Fig. 7c) reveal discretely configured multilayer’s in the two species: The high occupancy and high layer number of *M. rhetenor* creates an intense reflectivity that contrasts with the more diffusely coloured appearance of *M. didius*, in which an overlying second layer of scales effects strong diffraction.



FIGURE 6. *Morpho menelaus*. Image reproduced with permission under the terms of the GNU Free Documentation License.

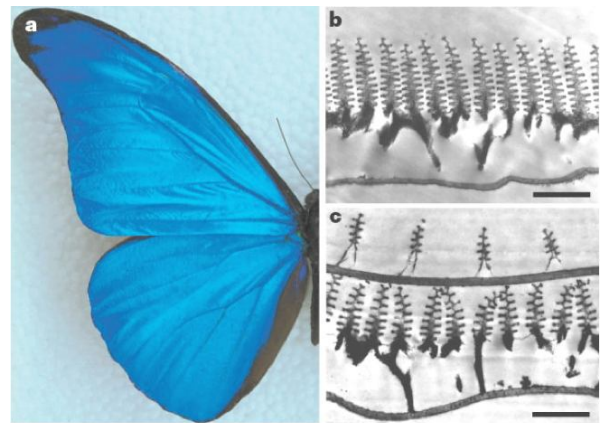


FIGURE 7. **a**, Real colour image of the blue iridescence in a *Morpho rhetenor* wing. **b**, **c**, Transmission electron microscopy reveals Christmas tree-like structures with characteristic dimensions on the order of some hundreds of nanometers in *M. rhetenor* (**b**) and *M. didius* (**c**). Scale bars, **b**, 1.8 μm ; **c**, 1.3 μm [9]. Image reproduced with permission. Image © 2003, Nature Publishing Group.

In the emerald-patched cattleheart (*Parides sesostris*) a photonic crystal is responsible for the green colour (for *Parides sp.* see Fig. 8). Scanning electron microscopy of the exposed photonic crystal after the superficial ridging has been removed reveals a reverse photonic crystal structure (Fig. 9) [9]. Transmission electron microscopy reveals neighbouring differently oriented domains of identical 3D structure that are distinguished by contrasting 2D patterns (here, the darkly contrasted material is cuticle) (Fig. 9).



FIGURE 8. *Parides* sp. Image reproduced with permission under a Creative Commons Attribution-Share Alike 2.5 Generic License.

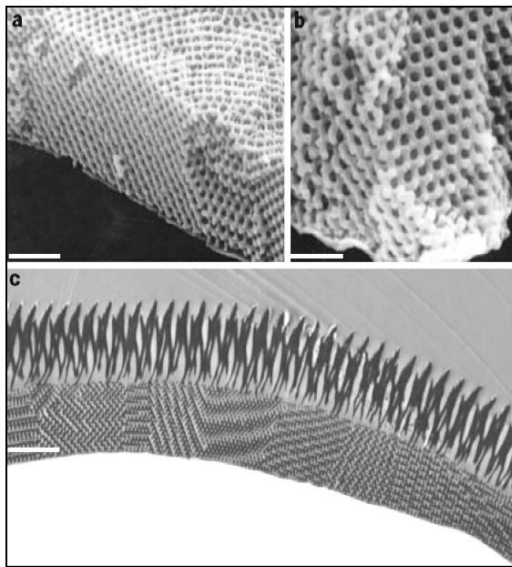


FIGURE 9. **a, b,** As revealed by scanning electron microscopy, an inverse photonic crystal creates the green colour of the emerald-patched cattleheart (*Parides sesostris*). **c,** transmission electron microscopy of a section through the scale shown in **a**. Scale bars, **a**, 1.2 μm ; **b**, 750 μm ; **c**, 2.5 μm . Inset: Specimen of *Parides sesostris*. [9]. Image reproduced with permission. Image © 2003, Nature Publishing Group.

White Butterflies

The white of the cabbage white butterfly (*Pieris rapae*, Fig. 10) is generated by small structures that are ornamented with elongated beads (Fig. 11 top and bottom left). These elongated beads scatter the incident light in all possible directions, resulting in white appearance of the butterfly.

Note the exquisite arrangement of the structures leading to the white: the nanoscale scattering beads are mounted on a regular scaffolding structure in the microscale. With current technological possibilities, it is possible to generate such exquisite structures.



FIGURE 10. A cabbage white (*Pieris rapae*). Note the little black spot on the wing – the nanostructure leading to black is shown in Fig. 12 bottom right. Image reproduced with permission under a Creative Commons Attribution-Share Alike 3.0 Unported License.

However, the costs and time invested would be exorbitantly high. The butterfly just eats some nectar and pollen, drinks some water and converts energy provided by the sun. Furthermore, it is self-replicating, producing hundreds of such “structures” in short time. This efficient way of producing nanostructures shows us clearly how much we could learn from nature.

The right part of Fig. 11 bottom shows how the little black dot on the cabbage white wing gets its black: the base structure is the same as in the white areas of the wing, but the elongated beads are missing. Therefore light is not reflected or scattered, but absorbed – the little dot appears black (although it is made from the same material as the surrounding white).

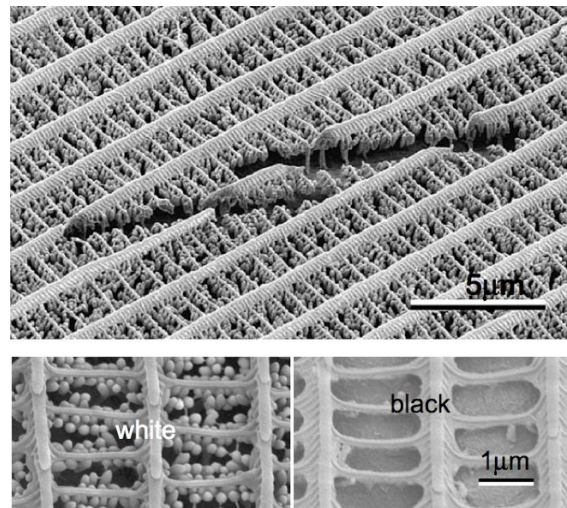


FIGURE 11. Scanning electron microscopy images of the microstructures from the cabbage white butterfly wing. **a,** The structures responsible for white. Scale bar 5 μm . **b,** The structures responsible for white (left) and black (right) [18]. Image reproduced with permission. Image © 2004, The Royal Society.

Peacock Feathers

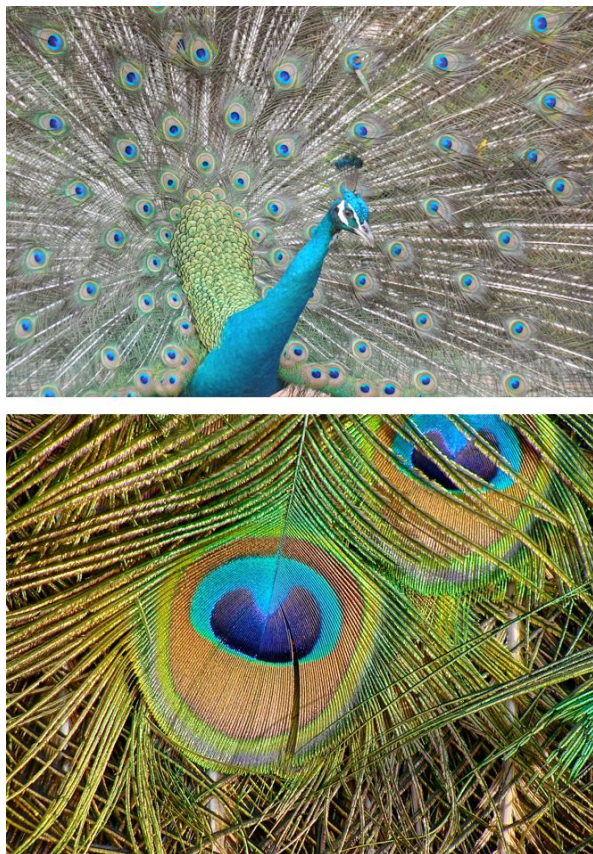


FIGURE 12. Top: Peacock. Bottom: Peacock feathers, Bottom image reproduced with permission under the terms of the GNU Free Documentation License.

The colour of the peacock feather (Fig. 12) has been source of attraction for scientists for more than 300 years, when Sir Isaac Newton correlated them with the colours of the interference patterns caused by the reflection of light between two surfaces (Newton's rings) [16]. Even earlier observations of peacock feathers were carried out by Hooke in 1665 [15]. However, it took until the 20th century until the structures responsible for the coloration were identified with scanning electron microscopy.

A Fabry-Pérot type of interferometer (Fig. 13) is responsible for the colour generation in peacock feathers (Figs. 11 and 12). A Fabry-Pérot etalon (Fig. 13) causes interference between the multiple reflections of light between two reflecting surfaces.

Constructive interference occurs if the transmitted beams are in phase, and this corresponds to a high-transmission peak of the etalon.

If the transmitted beams are out-of-phase, destructive interference occurs and this corresponds to a transmission minimum. Whether the multiply reflected beams are in-phase or not depends on the

wavelength (λ) of the light (in vacuum), the angle the light travels through the etalon (θ), the thickness of the etalon (l) and the refractive index of the material between the reflecting surfaces (n).

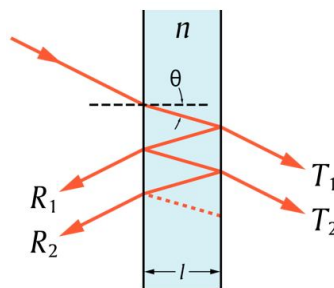


FIGURE 13. A Fabry-Pérot etalon. Light enters the etalon and undergoes multiple internal reflections. Image reproduced with permission under the terms of the GNU Free Documentation License.

Light is reflected on the front and backside of the structures in the peacock feather, whereby colour in a specific wavelength range is enhanced [19]. The colour generating structures in the peacock feather are made from melanin and have a photonic crystal like shape.

The distance between the single melanin cylinders determines the main colour in the respective region of the peacock feather: in the blue area the distance is 140 nanometres, in the green area 150 nanometres and in the yellow area 165 nanometres. The melanin structures are embedded in larger spike-like structures. These spikes are made from keratin, which is the main material of skin, hair, fingernails, hoofs and horns. In the case of the peacock feather, as opposed to, e.g., fingernails, the keratin spikes include the melanin cylinders: in the green region about 10 rows, and in the yellow region about 6 rows [19].

Iridescent Plants and Fruits

Like in animals, the most common mechanisms in plants are multilayer interference and diffraction gratings. The primary function of these colours in animals is signalling between members of the same species and camouflaging animals against their predators. Multilayer interference is found in plants, predominantly in shade-plant leaves, suggesting a role either in photo protection or in optimizing capture of photo synthetically active light [20]. Surprisingly, diffraction gratings may be a common feature of petals, and recent work has shown that bees use them as cues to identify rewarding flowers. Structural colour may be surprisingly frequent in the plant kingdom, playing important roles alongside pigment colour, however

still much more thing remains to be discovered about its distribution, development, and function [5].

The “peacock” fern *Selaginella willdenowii* is a common plant in the Malaysian rainforests. The photo shown in Fig. 14 was taken in the Bukit Wang Recreational Forest in Malaysia. The photo was taken with very long exposure time, as to show the blue colour of the leaves. Seen with the naked eye, the fern is bluish and seems to glow in semi-darkness.



FIGURE 14. The “peacock” fern *Selaginella willdenowii*, a common plant in the Malaysian rainforest. © Mr. Foozi Saad, IPGM, Malaysia. Image reproduced with permission.

In two *Selaginella* species, including *S. willdenowii*, interference results from the separation of two reflective lamellae in the outer wall of the epidermis [21, 22]. *S. willdenowii* is abundant in the Malaysian rainforest. Holding and tilting the leaf results in colour change from green to nearly total blue, although not as strong as seen in the long-exposure time photograph shown in Fig. 14. Some more ferns that show iridescence are *Danaea nodosa*, *Trichomanes elegans* and *Diplazium tomentosum* (Fig. 15). Iridescence also occurs in the flowering plants *Phylagathis rotundifolia* and *Begonia pavonina* and the iridescent algae *Dictyota mertensii* and *Ochtodes secundiramea*, as well as the blue fruits *Elaeocarpus angustifolius* and *Delarbreia michieana* [23].

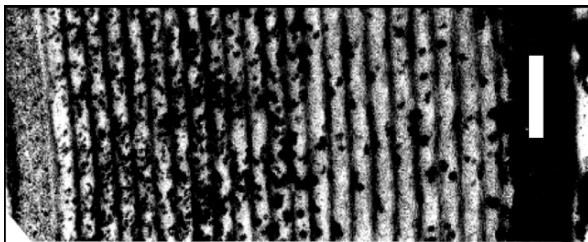


FIGURE 15. Ultrastructure of a *Diplazium tomentosum* leaf. Scale bar 0.5 μm [20]. Image reproduced with permission, © 1996, Botanical Society of America.

MATERIALS AND METHODS

A carpenter bee (*Xylocopa sp.*) with body length of 2.5 cm and a body width of 1.3 cm that was found dead at the UKM campus in Bangi, Malaysia, served as specimen in the investigations. It shows iridescent colours on its wings,

The nanostructures of the bee wing were investigated with non-contact atomic force microscopy (AFM, Park Systems XE-100), using a Silicon nitride cantilever with a spring constant of 40 N/m and a resonance frequency of 300.000 kHz.

The green and purple areas of the wing were identified visually, and a surgical scalpel was used to cut out various 2*2 mm² parts from inside the wing.

Samples were mounted with double side adhesive tape on round metal disks and mounted on the sample stage of the AFM. The whole instrument was mounted on an active vibration insulation table and inserted in an acoustic chamber, to minimise vibrations during the data acquisition. Images were acquired with a scan rate of 0.3 Hz in ambient conditions, at room temperature.



FIGURE 16. The Malaysian bee with the iridescent structural colours on its wings: a carpenter bee (*Xylocopa violacea*) with 2.5 cm body length and 1.3 cm body width.

Carpenter Bee

Carpenter bees (genus *Xylocopa*, in the subfamily *Xylocopinae*, Figs. 16 and 17) are large, hairy bees distributed worldwide. There are near 500 species of carpenter bee in 31 subgenera [24]. Their name comes from the fact that nearly all species build their nests in burrows in dead wood, bamboo, or structural timbers (except those in the subgenus *Proxylocopa*, which nest in the ground). Members of the related genus *Ceratinini* are sometimes referred to as “small carpenter bees” [24].



FIGURE 17. Carpenter bee (*Xylocopa sp.*). Note the purple and green areas on the wings. The wing coloration is iridescent, i.e., changes with the viewing angle. Image reproduced with permission from TrekNature ID nagaraj vn.

RESULTS

Visual Investigation

Wings have different patterns and colours: on the topside, purple and green areas can be identified. On the bottom side, the whole wing is purple. In intense light, the coloration of the topside of the wings changes with the viewing angle: in extreme positions, the whole topside of the wing exhibits green or purple. The abdomen is of a shiny black. Experiments with water droplets reveal that the whole body is water resistant and self-cleaning. When a droplet of water is placed on the coloured wings, the coloration disappears, indicating structural colours. Tearing the wings of the specimen under a dissecting microscope reveals a layered structure of the wing – this has also been confirmed by AFM scans (Fig. 18 top).

AFM Observations

AFM non-contact mode scans (AFM, Park Systems XE-100) in an area of the bee wing showing green coloration in Fig. 16 reveal at least three layers of the wing, with the top layers on each side being about 100 nm high (Fig. 18 top).

Note that the coloration in the AFM images shown in Figs. 18, 19 and 20 indicates height and not the coloration of the sample. Blue indicates the lowest parts of the specimen, white intermediate height and brown indicates the highest surface parts.

The brain-like structures on the top layer and on the second layer have a thickness of some hundreds of nanometres. This observation rules out thin films as the structures yielding the coloration.

AFM non-contact mode scans of the top layer of wing parts from the purple and the green area reveal two distinctively different types of nanostructures in the areas corresponding to the respective coloration (Figs. 19 and 20).

In the purple parts of the bee wing, the structures are less uniform concerning their widths and heights than in the green parts of the bee wing (Fig. 19). In the purple parts, the height of the structures is about 100 nanometres, whereas in the green part the structures are about 200 nanometres high (Fig. 20).

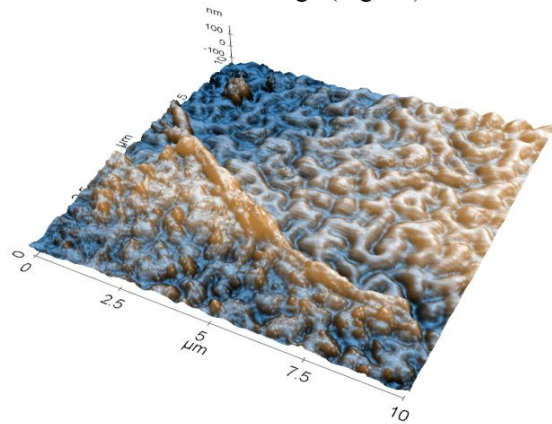


FIGURE 18. Top: AFM topography image revealing the layered structure of the bee wing. Bottom: Corral (brain-like structure). Image used with permission. © flickr ID purplemaniac.

DISCUSSION AND OUTLOOK

The presented first AFM images of the surface structures in areas of different coloration (purple and green) of the carpenter bee wing show distinct differences between the areas with different coloration. Further studies with AFM and scanning electron microscopy shall be performed on wing parts of the purple and green area with the top layer peeled off and on freeze fractured samples.

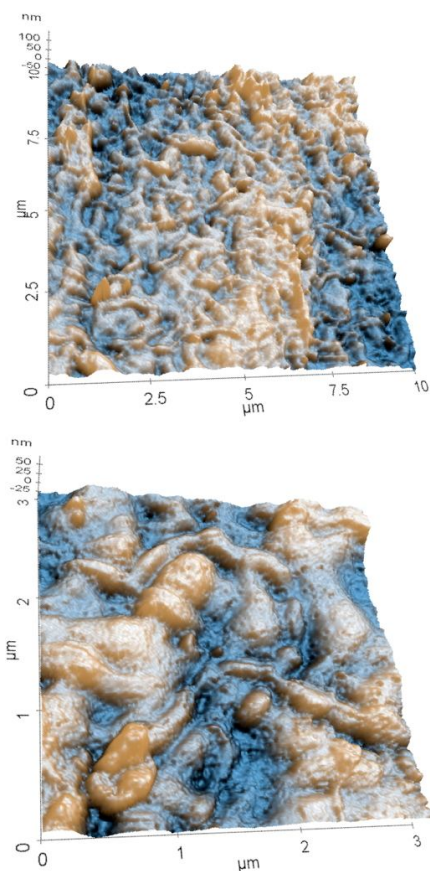


FIGURE 19. AFM topography image of the purple part of the bee wing. Top: Scan size $10 \times 10 \mu\text{m}^2$, bottom: Zoom, scan size $3 \times 3 \mu\text{m}^2$. The nanostructures of the wing were recorded via non-contact mode atomic force microscopy.

Brain-like shapes as the ones observed in the green part of the Carpenter bee wing (Fig. 18 top) can be found in various organisms, such as coralls (Fig. 18 bottom), Osage oranges (also known as hedge apples), in walnuts and the brain itself. Also in nanotechnology, the production of brain-like nanostructured polyaniline has been reported [25].

General investigations on common principles and advantages of brain-like structures in animated nature are currently not available. It would be interesting to compare various brain-like structures in nature, extract their deep principles and identify possible technological applications and advantages of such structures. Such a biomimetic approach, where knowledge transfer takes place from nature to the world of technology can provide innovative solutions for current technological challenges [26-29]. This approach can result in innovative new technological constructions, processes and developments. Biomimetics is a growing field that has the potential to drive major technical advances [30].

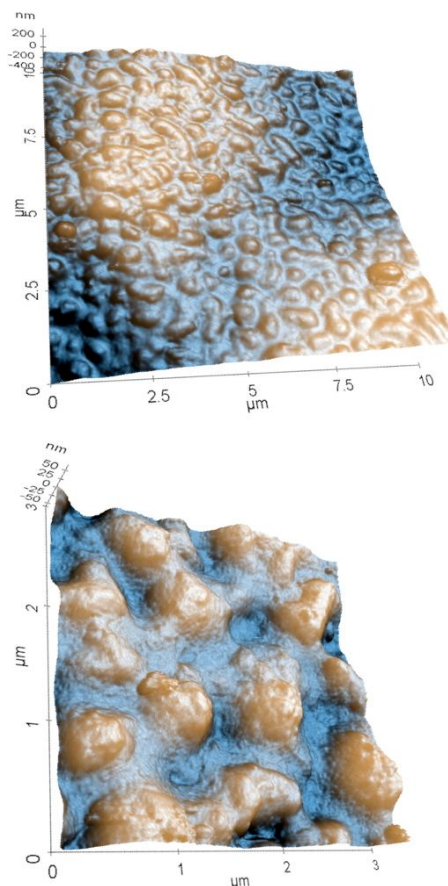


FIGURE 20. AFM topography image of the green part of the bee wing. Top: Scan size $10 \times 10 \mu\text{m}^2$, bottom: Zoom, scan size $3 \times 3 \mu\text{m}^2$. The nanostructures of the wing were recorded via non-contact mode atomic force microscopy.

Further investigation concerning the colour-generating structures in the carpenter bee wing will have to deal with the multi-functionality of the structures seen. The nanostructures in the bee wing serve various functions (such as for example self-repair, colour generation, water resistivity, self-cleaning). Extracting the deep principles concerning the colour generation will assist future man-made production of such colours. Since structural colours do not bleach, and no dyes are involved in the production process, various technological applications, e.g., in clothing production (such as batik) and smart colours for sensing applications, security labelling (such as spotting fake bank notes, [25]) or the manufacture of dynamic and vivid paints and coatings can be envisaged [32].

General principles that can be applied by engineers who are not at all involved in biology are e.g., integration instead of additive construction, optimization of the whole instead of maximization of a single component feature, multi-functionality instead of mono-functionality, energy efficiency and development via trial-and-error processes [28].

ACKNOWLEDGMENTS

The Austrian Society for the Advancement of Plant Sciences funded part of this work via the Biomimetics Pilot Project 'BioScreen'. Living in the tropics and exposure to high species diversity at frequent excursions to the tropical rainforests is a highly inspirational way to do biomimetics. Profs. F. Aumayr, H. Störi and G. Badurek from the Vienna University of Technology are acknowledged for enabling ICG three years of research in the inspiring environment in Malaysia. Crest (M) Sdn. Bhd. is acknowledged for instrumental support.

REFERENCES

1. S. Kinoshita, *Structural Colors in the Realm of Nature*, Singapore: World Scientific Publishing (2008).
2. S. Kinoshita and S. Yoshioka, "Structural colors in Nature: The role of regularity and irregularity in the structure", *ChemPhysChem* **6**, 1442-1459 (2005).
3. S. Kinoshita, S. Yoshioka and J. Miyazaki, "Physics of structural colors", *Rep. Prog. Phys.* **71**, 076401 (2008).
4. A. E. Seago, P. Brady, J.-P. Vigneron and T. D. Schultz. "Gold bugs and beyond: a review of iridescence and structural colour mechanisms in beetles (*Coleoptera*)", *J. Roy. Soc. Interface* **6**, 165-184 (2008).
5. B.J. Glover and H.M. Whitney, "Structural colour and iridescence in plants: the poorly studied relations of pigment colour", *Ann. Botany* **105**, 505-511 (2010).
6. A.R. Parker and N. Martini. "Structural colour in animals - simple to complex optics", *Opt. Laser Technol.* **38**, 315-322. (2006).
7. D.C. Giancoli, *Physics for Scientists and Engineers with Modern Physics*, 3rd ed., Upper Saddle River: Prentice Hall (2000).
8. A.R. Parker, "515 million years of structural colour", *J. Opt. A: Pure Appl. Opt.* **2**, R15-R28 (2000).
9. P. Vukusic and J. Roy Sambles, "Photonic structures in biology", *Nature* **424**, 852-855 (2003).
10. P. Vukusic and D.G. Stavenga, "Physical methods for investigating structural colours in biological systems", *J. Roy. Soc. Interface* **6**, 133-148 (2009).
11. M. Srinivasarao, "Optics in the biological world: Beetles, butterflies, birds and moths", *Chem. Rev.* **99**, 1935-1961 (1999).
12. J. Huxley, "The coloration of *Papilio zalmoxis* and *P. antimachus*, and the discovery of Tyndall blue in butterflies", *Proc. Roy. Soc. Lond. B* **193**, 441-453 (1976).
13. R.H. Lipson and C. Lu, "Photonic crystals: a unique partnership between light and matter", *Eur. J. Phys.* **30**, 33-48 (2009).
14. J.-M. Lourtioz, H. Benisty, V. Berger, J.-M. Gerard, D. Maystre and A. Tchelnokov, *Photonic Crystals: Towards Nanoscale Photonic Devices*, 2nd ed., Berlin Heidelberg: Springer Verlag (2008).
15. R. Hooke, *Micrographia: or, Some Physiological Descriptions of Minute Bodies Made by Magnifying Glasses*, 1st ed., London: J. Martyn and J. Allestry, 1665
16. I. Newton, "Opticks", London 1704 (numerous subsequent editions)
17. R.O. Prum, T. Quinn and R.H. Torres, "Anatomically diverse butterfly scales all produce structural colours by coherent scattering", *J. Exp. Bio.* **209**, 748-765 (2006).
18. D.G. Stavenga, S. Stowe, K. Siebke, J. Zeil and K. Arikawa, "Butterfly wing colours: Scale beads make white pierid wings brighter", *Proc. Roy. Soc. Lond. B* **271**, 1577-1584 (2004).
19. J. Zi, X. Yu, Y. Li, X. Hu, C. Xu, X. Wang, X. Liu and R. Fu, "Coloration strategies in peacock feathers", *Proc. Natl. Acad. Sci.* **100**, 12576-12578 (2003).
20. K.S. Gould and D.W. Lee, "Physical and ultrastructural basis of blue leaf iridescence in four Malaysian understory plants", *Am. J. Bot.* **83**, 45-50 (1996).
21. D.W. Lee and J.B. Lowry, "Physical basis and ecological significance of iridescence in blue plants", *Nature* **254**, 50-51 (1975).
22. C. Hebant and D.W. Lee, "Ultrastructural basis and developmental control of blue iridescence in Selaginella leaves", *Am. J. Bot.* **71**, 216-219 (1984).
23. D. Lee, *Nature's Palette*, Chicago: The University of Chicago Press (2000).
24. R.L. Minckley, "A cladistic analysis and classification of the subgenera and genera of the large carpenter bees, tribe Xylocopini (Hymenoptera: Apidae)". Scientific Papers, Natural History Museum, University of Kansas **9**, 1-47, 1998
25. Y. Zhu, J. Li, M. Wan, L. Jiang and Y. Wei, "A new route for the preparation of brain-like nanostructured polyaniline", *Macromol. Rapid Commun.* **28**, 1339-1344 (2007).
26. I.C. Gebeshuber and M. Drack, "An attempt to reveal synergies between biology and engineering mechanics", *Proc. IMechE Part C: J. Mech. Eng. Sci.* **222**, 1281-1287 (2008).
27. J. Benyus, *Biomimicry: Innovation Inspired by Nature*, New York, NY, USA: William Morrow & Company, Inc. (1997).
28. I.C. Gebeshuber, P. Gruber and M. Drack, "A gaze into the crystal ball: biomimetics in the year 2059", *Proc. IMechE Part C: J. Mech. Eng. Sci.* **223**, 2899-2918 (2009).
29. I.C. Gebeshuber, H. Stachelberger, B. A. Ganji, D. C. Fu, J. Yunas and B. Y. Majlis, "Exploring the innovational potential of biomimetics for novel 3D MEMS", *Adv. Mater. Res.* **74**, 265-268 (2009).
30. I.C. Gebeshuber, B.Y. Majlis and H. Stachelberger, "Tribology in biology: biomimetic studies across dimensions and across fields", *Int. J. Mech. Mat. Eng.* **4**, 321-327 (2009).
31. M. Kolle, P.M. Salgard-Cunha, M.R.J. Scherer, F. Huang, P. Vukusic, S. Mahajan, J.J. Baumberg and U. Steiner, "Mimicking the colourful wing scale structure of the *Papilio blumei* butterfly", *Nature Nanotechnology*, May 2010, advanced online publication
32. H. Kim, J. Ge, J. Kim, S. Choi, H. Lee, W. Park, Y. Yin and S. Kwon, "Structural colour printing using a magnetically tunable and lithographically fixable photonic crystal", *Nature Photonics* **3**, 534-540 (2009).